

# Optical terahertz wave generation in a planar GaAs waveguide

K. L. Vodopyanov<sup>1,\*</sup> and Yu. H. Avetisyan<sup>2</sup>

<sup>1</sup>Edward L. Ginzton Laboratory, Stanford University, Stanford, California 94305, USA

<sup>2</sup>Department of Microwave Engineering and Communication, Radiophysics Faculty, Yerevan State University, Yerevan, 375049 Armenia

\*Corresponding author: vodopyan@stanford.edu

Received July 23, 2008; revised August 26, 2008; accepted August 27, 2008;  
posted September 9, 2008 (Doc. ID 99049); published October 9, 2008

We report generation of terahertz (THz) radiation in a planar 61- $\mu\text{m}$ -thick GaAs waveguide with a  $\text{TM}_0$  propagation mode, achieved by phase-matched difference frequency mixing. The THz output was centered near 2 THz and had 1  $\mu\text{W}$  average power. As a pump source we utilized both the signal and the idler outputs of a near-degenerate type II synchronously pumped optical parametric oscillator operating near 2  $\mu\text{m}$  with the average powers of 250 and 750 mW, correspondingly. © 2008 Optical Society of America  
OCIS codes: 190.2620, 190.4410, 230.7370.

Photonic methods of terahertz (THz) generation are appealing owing to the availability of efficient diode-pumped lasers that can be used as a pump source. These lasers have a small size, can operate in different temporal formats, and are power scalable. GaAs is one of the least absorbing electro-optic (EO) crystals at THz frequencies (with an absorption coefficient  $<5 \text{ cm}^{-1}$  below 3 THz) and has several additional advantages that make it a good candidate for nonlinear optical THz generation, namely, small mismatch between the optical group ( $n_g \sim 3.4$  at 2  $\mu\text{m}$ ) and THz ( $n_{\text{THz}} \sim 3.6$ ) refractive indices, large second-order susceptibility, large thermal conductivity, and well-established fabrication techniques. Several schemes for producing high-peak- and high-average-power THz output by means of difference frequency generation (DFG) in GaAs were implemented recently: THz pulses with 2 MW peak power near 1 THz were achieved by noncollinear DFG in bulk GaAs [1], and a quasi-continuous (50 MHz repetition rate) THz source based on cavity-enhanced DFG in orientation-patterned GaAs was demonstrated with the average power of 1 mW at 2.8 THz [2].

Guided-wave interactions confine radiation to transverse dimensions of the order of a THz wavelength or less over the whole length of the EO crystal, thus lifting the trade-off between confinement and diffraction. DFG THz efficiency can be noticeably enhanced in this case, since it critically depends on the confinement of interacting fields; in addition, in a waveguide (WG), phase matching can be achieved with optically isotropic materials such as GaAs and GaP, owing to the WG dispersion added to that of a bulk crystal [3,4]. In a pioneering work by Thompson and Coleman, THz output from a planar GaAs WG ( $\text{TE}_0$  mode) was achieved with a nanowatt range average power ( $\sim 1 \text{ mW}$  peak) by mixing various pairs of laser lines from two separate  $\text{CO}_2$  lasers [3]. Lately, phase-matched THz generation was demonstrated in channel GaP waveguides with 1- $\mu\text{m}$  optical pumping, both via DFG using nanosecond pulses [5] and optical rectification with femtosecond pulses [6]. In this Letter, we demonstrate phase-matched

THz generation in a planar GaAs WG using a dual-wavelength pump source near 2  $\mu\text{m}$ .

In the limit of small conversion and long pulses, the power  $P_1$  at the difference (THz) frequency in a WG scales as [7]

$$P_1 \sim (d_{\text{eff}}^2/n_{\text{opt}}^2 n_{\text{THz}}) L^2 P_2 P_3, \quad (1)$$

where  $P_2$  and  $P_3$  are optical pump powers,  $d_{\text{eff}}$  is an effective nonlinear coefficient,  $n_{\text{opt}}$  and  $n_{\text{THz}}$  are optical and THz refractive indices, and  $L$  is a length of the crystal. If we assume that the optimized  $L$  is of the order of  $1/\alpha_{\text{THz}}$ , where  $\alpha_{\text{THz}}$  is the THz power absorption coefficient, we can introduce a THz DFG figure of merit (FOM) for a WG,

$$\text{FOM} = d_{\text{eff}}^2 / (n_{\text{opt}}^2 n_{\text{THz}} \alpha_{\text{THz}}^2). \quad (2)$$

Table 1 compares optical and THz properties, as well as FOMs, for GaAs, GaP, and  $\text{LiNbO}_3$  crystals [8,9]. One can see that GaAs has the largest FOM for WG frequency conversion, primarily owing to its small THz absorption. In addition, as we will see below, GaAs has a “convenient” mismatch between  $n_g$  and  $n_{\text{THz}}$ : on the one hand, a WG designed for phase-matched DFG operates far from the cutoff regime; on the other hand, it does not support propagation of the higher-order modes.

As a dual-wavelength pump source we used the output of a near-degenerate optical parametric oscillator (OPO), based on a type II periodically poled lithium niobate (PPLN) crystal and synchronously pumped by a mode-locked Nd:YVO<sub>4</sub> laser with pulse duration of 7 ps, at a repetition rate 50 MHz [2,10]. The singly resonant OPO generated two closely spaced narrow-linewidth “signal” and “idler” wavelengths (with the resonant “signal”), with the frequency spacing variable between 0 and 4 THz by changing PPLN temperature. The signal and the idler outputs were collinear to each other and were extracted using a thin-film polarizer inside the OPO cavity; the angle of incidence on the polarizer was adjusted to optimize the outcoupling efficiency. The av-

**Table 1. Linear, Nonlinear Optical, and THz Properties, as Well as FOMs, for GaAs, GaP, and LiNbO<sub>3</sub> Crystals<sup>a</sup>**

	GaAs	GaP	LiNbO <sub>3</sub>
THz nonlinear coefficients, <sup>b</sup> $d_{\text{eff}}$ (pm/V)	46	22	152
THz absorption at 1–2 THz (cm <sup>-1</sup> )	1	3.3	22
Optical reference index, $n(\text{opt})$	3.33 at 2 $\mu\text{m}$	3.11 at 1 $\mu\text{m}$	2.16 at 1 $\mu\text{m}$
THz reference index, $n(\text{THz})$	3.6	3.3	5.2
Figure of merit	53	1.4	2

<sup>a</sup>References [8,9].<sup>b</sup>THz nonlinear coefficients  $d_{\text{eff}}$  were derived from EO coefficients.

erage powers in the signal and idler waves were 250 and 750 mW, correspondingly.

The planar GaAs waveguide was 7.5 mm long and 8 mm wide and had a thickness of  $d=61\pm 1\ \mu\text{m}$ ; it was fabricated from an undoped semi-insulating GaAs wafer (AXT, Inc., resistivity  $>10^7\ \Omega\text{cm}$ , absorption at  $2\ \mu\text{m}<0.01\ \text{cm}^{-1}$ ) by optical polishing and cleaving end faces. No antireflection coating was applied. The THz radiation was generated by difference frequency mixing between orthogonally polarized OPO signal and idler waves. The signal and idler beams propagated along the  $[\bar{1}10]$  crystalline direction of GaAs with polarizations aligned along  $[001]$  and  $[110]$ , correspondingly. According to the GaAs symmetry, polarization of the generated THz  $E$  field has to be oriented along its  $[110]$  direction (Fig. 1) and therefore corresponds to the TM guiding mode of a planar WG.

The generated THz frequency was set in our case by the two pumping frequencies. The maximum THz output was determined by the phase-matching condition, i.e., equality of the optical  $n_g$  and the effective WG refractive index for the THz. Figure 2 shows the planar WG dispersion for GaAs for the lowest-order  $\text{TM}_m$  modes ( $m=0, 1, 2$ ) and  $d=61\ \mu\text{m}$ .

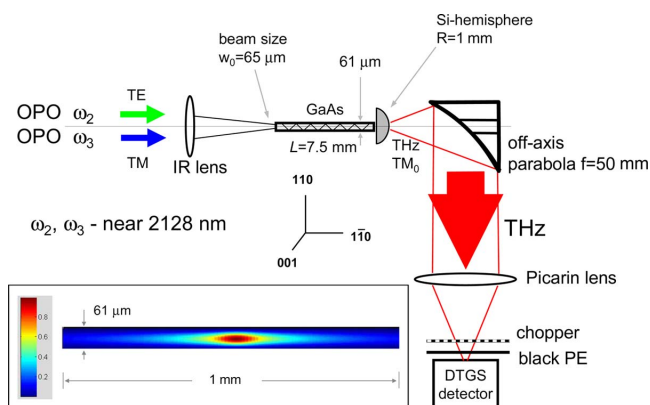


Fig. 1. (Color online) Schematic of the experiment. The signal ( $\omega_3$ ) and the idler ( $\omega_2$ ) beams from a near-degenerate (around 2128 nm) OPO are mixed in the GaAs WG to generate a THz wave through the DFG process  $\omega_1 = \omega_3 - \omega_2$ . The output is collimated by an off-axis parabolic mirror and detected using a room-temperature DLaTGS detector. Inset: calculated THz intensity distribution at the output face of the WG.

The collinear pump beams from the OPO were focused to a  $w=65\ \mu\text{m}$  beamspot ( $1/e^2$  intensity radius) at the front facet of the waveguide (Fig. 1). The coupling efficiency to the WG was calculated to be 45%, the losses arising mostly from the clipping and Fresnel reflection. A hemispherical silicon (Si) lens was attached to the WG to outcouple THz radiation to the free space. The THz output was collected by a 2 in. (50 mm) focal length, 1 in. (25 mm) diameter off-axis parabolic mirror (with a 3 mm hole to transmit optical beams) and detected using a Picarin lens and a room-temperature Bruker DLaTGS pyroelectric detector. Black polyethylene filters were used to block the optical radiation. The measured THz output was peaked at 2.07 THz, in excellent agreement with theoretical predictions. Figure 3 plots the THz output from the WG as a function of frequency. Also shown are calculated tuning curves for the  $\text{TM}_0$  mode,  $d=61\ \mu\text{m}$ ,  $\alpha_{\text{THz}}=3\ \text{cm}^{-1}$ , for the monochromatic pump (dotted curve) and for the pump with a finite ( $\sim 100\ \text{GHz}$ ) bandwidth (solid curve).

At the peak, the average output power was  $\sim 1\ \mu\text{W}$ , measured with our room-temperature detector, with a signal-to-noise ratio of  $\sim 100$ . We believe that the measured THz output corresponds to the fundamental  $\text{TM}_0$  mode, since the closest mode,  $\text{TM}_1$ , has an antisymmetric  $E$ -field distribution and therefore cannot be excited by the symmetric pump; in addition,

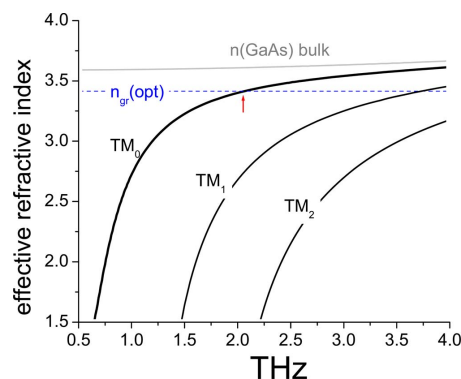


Fig. 2. (Color online) Planar GaAs WG dispersion for  $\text{TM}_m$  modes ( $m=0, 1, 2$ ) for  $d=61\ \mu\text{m}$ . Bulk GaAs THz dispersion (gray line) and group optical index ( $n_g$ ) for  $\lambda \approx 2.1\ \mu\text{m}$  (dashed line) are also shown. The arrow corresponds to the frequency where the phase-matching condition is achieved in our experiment.

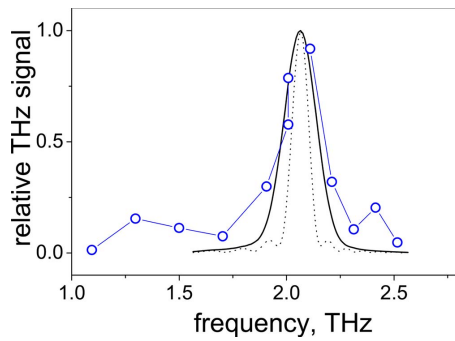


Fig. 3. (Color online) THz output from the WG as a function of frequency. Also shown are calculated tuning curves ( $TM_0$  mode,  $d=61\ \mu\text{m}$ ,  $\alpha_{\text{THz}}=3\ \text{cm}^{-1}$ ) for the monochromatic pump (dotted curve) and for the pump with a 100 GHz bandwidth (solid curve).

the  $TM_1$  mode is not phase matched. As for the  $TM_2$  mode, 2.07 THz is below its cutoff frequency (Fig. 2).

It should be noted that the 7 ps duration of our pump pulses was close to the optimal value, from the viewpoint of maximizing optical-to-THz conversion, while keeping the power density small. The pulse duration was such that the corresponding bandwidth was close to the phase-matching acceptance bandwidth of the GaAs WG. It follows from theory that making the pulses shorter than the optimal does not improve THz efficiency but increases the peak power and, as a result, the role of detrimental higher-order effects, such as self-phase modulation, multiphoton absorption, and others [11]. No degradation of the WG due to optical irradiation was observed, and the setup was able to run continuously for the unlimited time. In fact, the peak pump power density at the WG surface was only  $43\ \text{MW}/\text{cm}^2$ , which is 2 orders of magnitude smaller than that in [6].

To estimate theoretically the THz output, we assumed that the pump field distribution is unchanged over the WG length (near-field approximation). In contrast, we assumed that THz radiation is free to diffract along the  $y$  axis (in the plane of the WG) and is confined along the  $x$  axis (WG thickness), with the eigenmode distribution  $E_x \sim \cos(hx)$ , where  $h \approx \pi/d$ , and  $x=0$  corresponds to the center of the WG. The crystal was divided into slices along the  $z$  axis (propagation direction), and the THz field at the output WG facet was found numerically by coherently adding solutions to the wave equation with nonlinear polarization at each slice acting as a source. THz absorption was taken into account. The inset to Fig. 1 shows the calculated intensity at the WG output. When several reduction factors were considered, due to (i) optical beam clipping, (ii) Fresnel losses, and (iii) finite spectral width of the optical pump, the calculated THz average power amounted to  $4\ \mu\text{W}$ . A factor of 4 between theory and experiment ( $1\ \mu\text{W}$ ) can be attributed to

our less-than-unity THz collection efficiency to the detector.

Confining interacting waves in two, rather than one dimension, e.g., in a rodlike WG (with the confinement due to GaAs–air interfaces or to a photonic bandgap structure), will noticeably enhance THz output. Calculations show that the DFG efficiency in a  $61 \times 65\ \mu\text{m}$  cross section WG is expected to be  $\sim 20$  times larger than in our planar WG. Further improvement can be accomplished through eliminating optical Fresnel losses and optimization of the pump focusing. Achieving 1 mW of average THz power in such a WG will require, in the temporal format of our present experiment, average optical powers of  $\sim 2\ \text{W}$  in each beam.

In conclusion, we have demonstrated a microwatt range THz source with a bandwidth of  $\sim 100\ \text{GHz}$ , based on a planar GaAs waveguide using a compact dual-wavelength pump source operating near  $2\ \mu\text{m}$  with a moderate average and peak power. Confining interacting beams in two dimensions in our future work is expected to improve optical-to-THz conversion efficiency by almost 2 orders of magnitude. Covering a wide spectral range can be achieved by using an array of waveguides with a variable cross section.

We thank Joe Schaar for help in the experiment and Tim Brand for fabricating the WG samples (both at Ginzton Laboratory, Stanford University). This work was supported by the Defense Advanced Research Projects Agency (DARPA) (grant FA9550-04-1-0465) and by the Ministry of Education and Science of Armenia.

## References

1. S. Ya. Tochitsky, J. E. Ralph, C. Sung, and C. Joshi, *J. Appl. Phys.* **98**, 026101 (2005).
2. J. E. Schaar, K. L. Vodopyanov, and M. M. Fejer, *Opt. Lett.* **32**, 1284 (2007).
3. D. E. Thompson and P. D. Coleman, *IEEE Trans. Microwave Theory Tech.* **22**, 995 (1974).
4. V. Berger and C. Sirtori, *Semicond. Sci. Technol.* **19**, 964 (2004).
5. J. I. Nishizawa, K. Suto, T. Tanabe, K. Saito, T. Kimura, and Y. Oyama, *IEEE Photon. Technol. Lett.* **19**, 143 (2007).
6. G. Chang, C. J. Divin, J. Yang, M. A. Musheinish, S. L. Williamson, A. Galvanauskas, and T. B. Norris, *Opt. Express* **15**, 16308 (2007).
7. E. J. Lim, H. M. Herka, M. L. Bortz, and M. M. Fejer, *Appl. Phys. Lett.* **59**, 2207 (1991).
8. K. L. Vodopyanov, *Laser Photonics Rev.* **2**, 11 (2008).
9. J. Hebling, A. G. Stepanov, G. Almasi, B. Bartal, and J. Kuhl, *Appl. Phys. B* **78**, 593 (2004).
10. J. E. Schaar, K. L. Vodopyanov, P. S. Kuo, M. M. Fejer, X. Yu, A. Lin, J. S. Harris, D. Bliss, C. Lynch, V. G. Kozlov, and W. Hurlbut, *IEEE J. Sel. Top. Quantum Electron.* **14**, 354 (2008).
11. K. L. Vodopyanov, *Opt. Express* **14**, 2263 (2006).